

Available online at [www.sciencedirect.com](http://www.sciencedirect.com)

Energy Procedia 1 (2009) 3515–3522

---

---

**Energy  
Procedia**

---

---

[www.elsevier.com/locate/procedia](http://www.elsevier.com/locate/procedia)

GHGT-9

## Core-scale experimental study of relative permeability properties of CO<sub>2</sub> and brine in reservoir rocks.

Jean-Christophe Perrin<sup>a,\*</sup>, Michael Krause<sup>a</sup>, Chia-Wei Kuo<sup>a</sup>, Ljuba Miljkovic<sup>a</sup>, Ethan Charoba, and Sally M. Benson<sup>a</sup>

<sup>a</sup>Department of Energy Resources Engineering, Stanford University, Stanford, CA 94305

---

### Abstract

Experimental studies of both drainage and imbibition displacements are needed to improve our fundamental understanding of multi-phase flow and trapping in CO<sub>2</sub>-brine systems and effectively take advantage of the large storage capacity of saline aquifers. Very few relative permeability measurements have been made and even fewer with *in situ* saturation measurements. Two new sets of steady state relative permeability measurements have been made in two different rock samples, and over a range of injection flow rates. These studies show that multi-phase brine displacement efficiency is strongly affected by the heterogeneity of the core. Moreover, we observe that, at any given fractional flow, different flow rates result in different CO<sub>2</sub> saturations. Similarly, different flow rates lead to different relative permeability curves. Numerical simulations of two phase displacement are performed on one sample, and at one fractional flow of CO<sub>2</sub>. Numerical simulations demonstrate that some of the features of the saturation distributions can be qualitatively replicated. However, improvements in the correlations between porosity, saturation and capillary pressure will be needed to replicate the saturation distributions measured in the experiments.

*Keywords:* Carbon Dioxide, Relative Permeability, Sequestration, X-Ray CT scanning.

---

© 2009 Elsevier Ltd. Open access under [CC BY-NC-ND license](https://creativecommons.org/licenses/by-nc-nd/4.0/).

### 1. Introduction

Carbon dioxide capture and storage can play an important role on reducing greenhouse gas emissions from stationary sources of emissions. The capacity for storing CO<sub>2</sub> resides in saline aquifers, which are both broadly distributed and have a tremendous amount of pore volume. Experimental studies of both drainage and imbibition displacements are needed to improve our fundamental understanding of multi-phase flow and trapping in saline aquifers and effectively take advantage of their large storage capacity. This paper describes core-scale measurements of steady-state CO<sub>2</sub>/brine displacement and relative permeability in two different rock samples over a range of flow rates. The experimental results are accompanied by some preliminary simulations of the core flood experiments. These fundamental studies will provide important insights about the footprint of CO<sub>2</sub> plumes, pressure buildup during injection, capillary trapping and leakage potential.

---

\* Corresponding author. Tel.: +1-650-723-0099; fax: +1-650-725-2099.  
E-mail address: [perrin@stanford.edu](mailto:perrin@stanford.edu).

## 2. Material and methods

### 2.1. Experimental setup

A new experimental facility has been designed in the Energy Resources Engineering Department at Stanford University for two-phase core flooding experiments (Figure 1). The facility allows for continuous injection of CO<sub>2</sub> and brine into rock cores at reservoir pressures and temperatures, while obtaining high resolution 3-dimensional maps of CO<sub>2</sub> and brine saturations. The core sample is wrapped in a heat-shrinkable Teflon sleeve and placed in an aluminum core holder. A pump (Pump D) injects water around the sleeve to create the overburden pressure (reservoir pressure). Two electric heaters warm the water inside the core holder to maintain the core at the reservoir temperature ( $T^{\text{res}}$ ). Two dual-pump systems are used to inject brine and CO<sub>2</sub> in the core sample (Pumps A1 & A2 for CO<sub>2</sub> and B1 & B2 for brine). Both of them are composed of two pumps connected with a set of electric valves. The dual pump configurations provide continuous fluid delivery by synchronizing the pump and refill strokes so that at least one pump is always delivering fluid. Electric valves support automated functions and are ideal for CO<sub>2</sub> application. The pumps can inject CO<sub>2</sub> and brine either at a constant volumetric flow rate or a constant pressure. The pumps can inject CO<sub>2</sub> and brine either at a constant volumetric flow rate or a constant pressure.

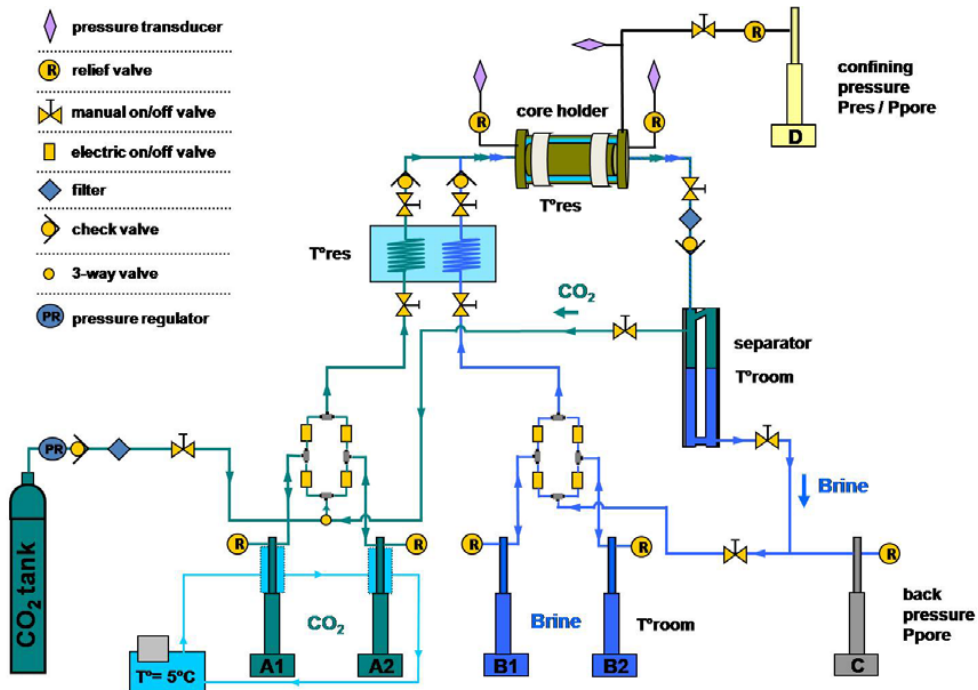


Figure 1: Schematic of the experimental setup developed in the Energy Resources Engineering department at Stanford University and used for two phase core flooding experiments.

The bodies of the CO<sub>2</sub> pumps are surrounded by water-cooled temperature jackets. Temperature jackets are maintained at a constant temperature of 5°C, which allows fast and complete filling and refilling of the cylinder when pumping the liquefied fluid and ensures a constant mass injection rate. Before entering the core, CO<sub>2</sub> and brine pass through a water bath (heat exchanger) to be heated at the reservoir temperature ( $T^{\text{res}}$ ). They are then mixed and co-injected into the core. After having flown through the core, CO<sub>2</sub> and brine are separated by gravity in a high pressure separator composed of a high pressure vessel adjacent to a heavy-duty high pressure liquid level

gauge. The liquid level gage is equipped with a transparent ½ inch thick glass which allows to measure and follow the height of the interface between brine and liquid CO<sub>2</sub> during the experiments. After the separator, the CO<sub>2</sub> returns back to the CO<sub>2</sub> pump system and the brine is conducted back to the brine pump system. Between the separator and the CO<sub>2</sub> pump system, another pump (Pump C) is used to maintain the back pressure in the system. The back pressure, also called pore pressure, is always at least 200 psi below the overburden pressure value in order to avoid any leakage through the Teflon sleeve surrounding the core. The dual-pump configuration allows for continuous experiments over week to months. In addition, the two fluids are in constant contact each other, ensuring that the CO<sub>2</sub> and brine are in thermodynamic equilibrium, thus avoiding inter-phase mass transport. This precaution is meant to avoid drying the core, which often happens when dry CO<sub>2</sub> is injected into a core. During the experiments, the pressure drop across the core is measured with two high resolution pressure transducers (~100 Pa). The temperature inside the core holder, the pressure drop, the injection flow rate, the injection pressure and the volume of each pump is measured and recorded by a data acquisition system. The entire setup, despite its size, is easily movable and can be transported to a room where X-ray CT scanning is used to measure CO<sub>2</sub> and brine saturations, in real time, inside the core sample.

## 2.2. Experimental procedure

### 2.2.1. Relative permeability measurements

Steady state relative permeability experiments are performed using the multi-phase flow facility described above. The rock samples are 2 in. (5.08 cm) diameter cylinders, with a maximum length of 8 in. (20.32 cm). The permeability of the core is first measured by injecting brine at several different flow rates while measuring the pressure drop across the core. The permeability is measured at the same temperature and pressure used during the multi-phase flow experiments. Using Darcy's law and knowing the viscosity of the brine solution at the experimental conditions ( $T^{\circ}_{res}$ ,  $P_{res}$ ), the permeability is calculated with a precision of 2 to 5%. To measure a drainage relative permeability curve (the core is initially fully saturated with the brine solution), CO<sub>2</sub> and brine are co-injected in different proportions (fractional flows). The fractional flow of CO<sub>2</sub>  $f_{CO_2}$  is defined as the ratio between the volumetric flow rate of brine-saturated CO<sub>2</sub> at reservoir conditions  $FR_{CO_2}^{T^{\circ}_{res}, P_{res}}$  and the total volumetric flow rate  $FR_{CO_2}^{T^{\circ}_{res}, P_{res}} + FR_{brine}^{T^{\circ}_{res}, P_{res}}$ :

$$f_{CO_2} = \frac{FR_{CO_2}^{T^{\circ}_{res}, P_{res}}}{FR_{CO_2}^{T^{\circ}_{res}, P_{res}} + FR_{brine}^{T^{\circ}_{res}, P_{res}}} \quad \text{Eq. 1}$$

For each fractional flow, the pressure drop across the core is measured as well as the CO<sub>2</sub> saturation in the core. When pressure drops and saturations have stabilized, steady state is achieved and both pressure and saturation are recorded. Steady state is generally reached after having injected 3 to 5 pore volumes of fluid. The data are always collected after at least 6 pore volumes. This procedure is repeated with sequentially higher fractional flows until 100% CO<sub>2</sub> is injected.

### 2.2.2. Measuring porosity and CO<sub>2</sub> saturation at the sub-core scale

The X-ray CT scanner creates 2-D saturation maps at different locations along the length of the sample. The 3-D saturation maps are then constructed by stacking the 2-D images along the third dimension. The X-Y resolution in the plane is 0.254 mm by 0.254 mm for the experiments that are discussed here. The image thickness varies from 1 to 3 mm, depending on the experiment. To obtain a porosity map of the core, two sets of images are needed: the dry images, when the sample is dry and the pore space is filled with air, and the brine saturated images, when the core is fully saturated with brine at the reservoir conditions. The porosity  $\Phi$  of each voxel element is then calculated using Eq. 2 [1]:

$$\Phi = \frac{CT_{\text{brine}}^{\text{sat}} - CT_{\text{dry}}}{CT_{\text{brine}} - CT_{\text{air}}} \quad \text{Eq. 2}$$

where CT is a numerical value converted from the X-ray attenuation coefficients. The CT numbers are normalized relative to the linear absorption coefficient of water [2].

To obtain the saturation map at each CO<sub>2</sub> fractional flow, three sets of images are needed: the brine saturated images, the CO<sub>2</sub> saturated images (the core is filled with CO<sub>2</sub> at reservoir conditions only) and the experimental images, at steady state, for the corresponding fractional flow. The CO<sub>2</sub> and brine saturations are then calculated for each voxel using [1]:

$$S_{\text{CO}_2} = \frac{CT_{\text{exp}} - CT_{\text{brine}}^{\text{sat}}}{CT_{\text{CO}_2}^{\text{sat}} - CT_{\text{brine}}^{\text{sat}}} \quad \text{and} \quad S_{\text{brine}} = 1 - S_{\text{CO}_2} \quad \text{Eq. 3}$$

### 2.3. Numerical Methods

The multi-phase flow simulator TOUGH2 MP with the ECO2N fluid property module [3] was used to try to replicate the laboratory experiments. TOUGH2 MP is the multiprocessor version of TOUGH2 - a numerical simulator for flows of multicomponent, multiphase fluids in porous media [4]. ECO2N was designed for applications in geologic sequestration of CO<sub>2</sub> in saline aquifers. It includes a comprehensive description of the thermodynamics and thermophysical properties of H<sub>2</sub>O - NaCl - CO<sub>2</sub> mixtures.

## 3. Results

### 3.1. Drainage in a heterogeneous sample from the Otway Basin

The rock sample is 8.3 cm long and was cored from the CRC1 well of the CO<sub>2</sub>CRC-Otway project, Australia, at a depth of 2071 m. A relative permeability experiment has been performed on this sample during the drainage phase. The total flow rate of 2 mL/min results in a flow velocity expected for a large scale CO<sub>2</sub> storage project in the region near the injection well. To mimic reservoir conditions, experiments were conducted at 63°C and a pressure of 12.4 MPa. The brine solution was composed of 6g/L NaCl and 0.5g/L CaCl<sub>2</sub>. The absolute permeability was measured at 50+/-2 mD and the mean porosity is 18.2%. The porosity and saturation maps were constructed by stacking 77 images, each image being 1mm thick. Figure 2a shows the slice-averaged porosity profile along the core and Figure 2b presents the 3D view of the porosity map. The porosity map demonstrates stratigraphic variations with a high degree of variability along the length of the core. As revealed by the 3D view, several low porosity layers with a small dip angle are present.

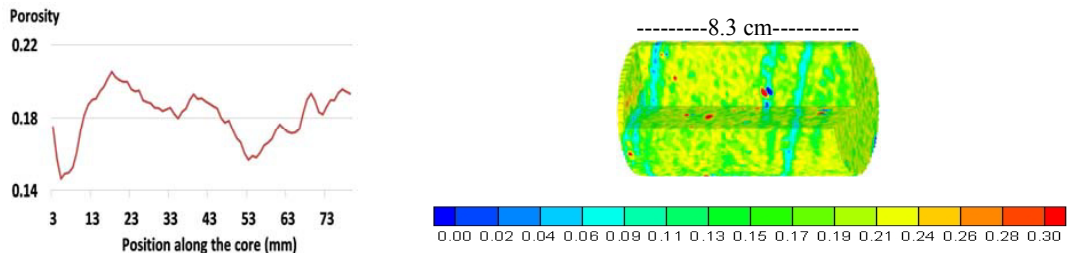


Figure 2:

a) Porosity profile along the core.

b) Three dimensional porosity map.

The steady state distribution of CO<sub>2</sub> saturations in the core at different fractional flows are shown in Figure 3. The spatial distribution of CO<sub>2</sub> inside the core is very heterogeneous. Steady state saturations mimic the stratigraphic features observed in the porosity map. Low porosity layers correspond to low CO<sub>2</sub> saturations and higher porosity regions have higher average CO<sub>2</sub> saturations. As observed on the slice averaged saturation profiles shown Figure 4a, the variability of CO<sub>2</sub> saturation along the core is important. No important end effects are visible since no visible general trend is seen close to the ends of the core. Similarly there are no obvious signs of gravity override of the less dense CO<sub>2</sub> phase, as would be indicated by lower CO<sub>2</sub> saturations at the bottom of the core.

The relative permeability curves measured on this sample during the drainage phase are plotted Figure 4b. Interestingly, the residual water saturation has an unusually high value (0.44). This inefficiency of the drainage was observed previously in a number of studies [5, 6], and Miljkovic et al. [7] concluded that sub core-scale heterogeneities could explain these observations.

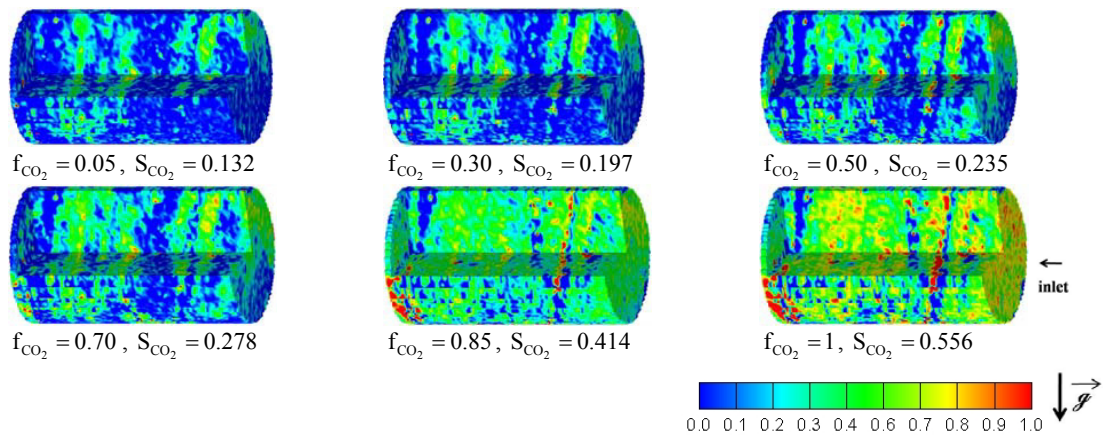


Figure 3: Three dimensional maps of CO<sub>2</sub> saturation inside the rock sample at steady state for different fractional flows of CO<sub>2</sub>. The CO<sub>2</sub> saturation is indicated below each image together with the corresponding fractional flow. The views show the core in its real orientation during the experiment, the gravity being oriented from top to bottom. The fluids were injected from right to left as indicated by the arrow at the right side of the 100% CO<sub>2</sub> fractional flow case.

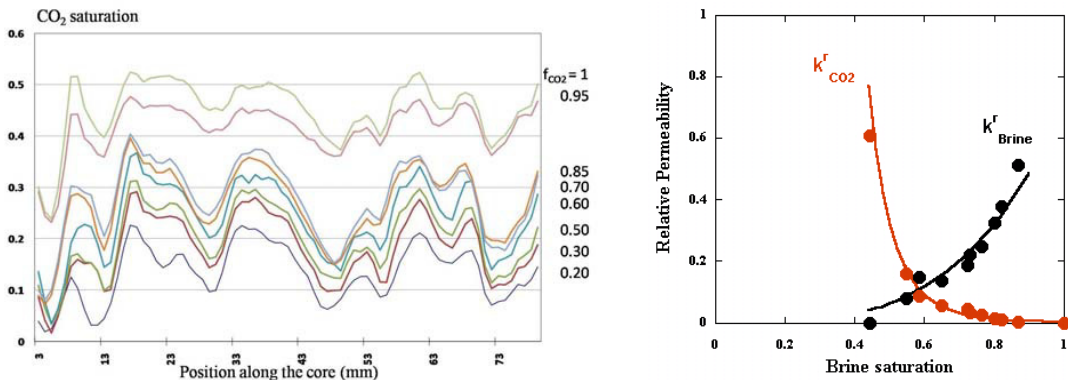


Figure 4:  
 a) CO<sub>2</sub> saturation profiles along the core for different fractional flows of CO<sub>2</sub>, from 0.20 to 1.  
 b) Relative permeability curves.

3.2. Drainage in a heterogeneous Berea sandstone.

The rock sample is 15.24 cm long, the average absolute permeability was measured at 430+/-7 mD and the average porosity is 20.3%. The porosity and saturation 3D maps were built by stacking 29 images. Figure 5a shows the slice-averaged porosity profile along the core and Figure 5b presents the three dimensional view of the porosity map. Measurements were made at 50°C and 12.4 MPa. Slice-averaged porosity values vary from 19.8% to 20.65%.

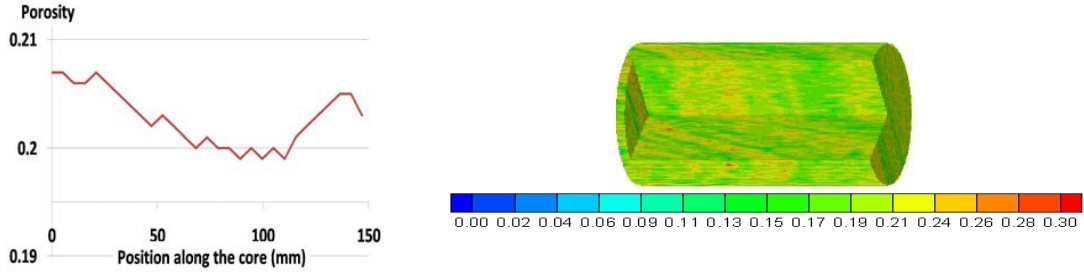


Figure 5:  
a) Porosity profile along the core.

b) Three dimensional porosity map.

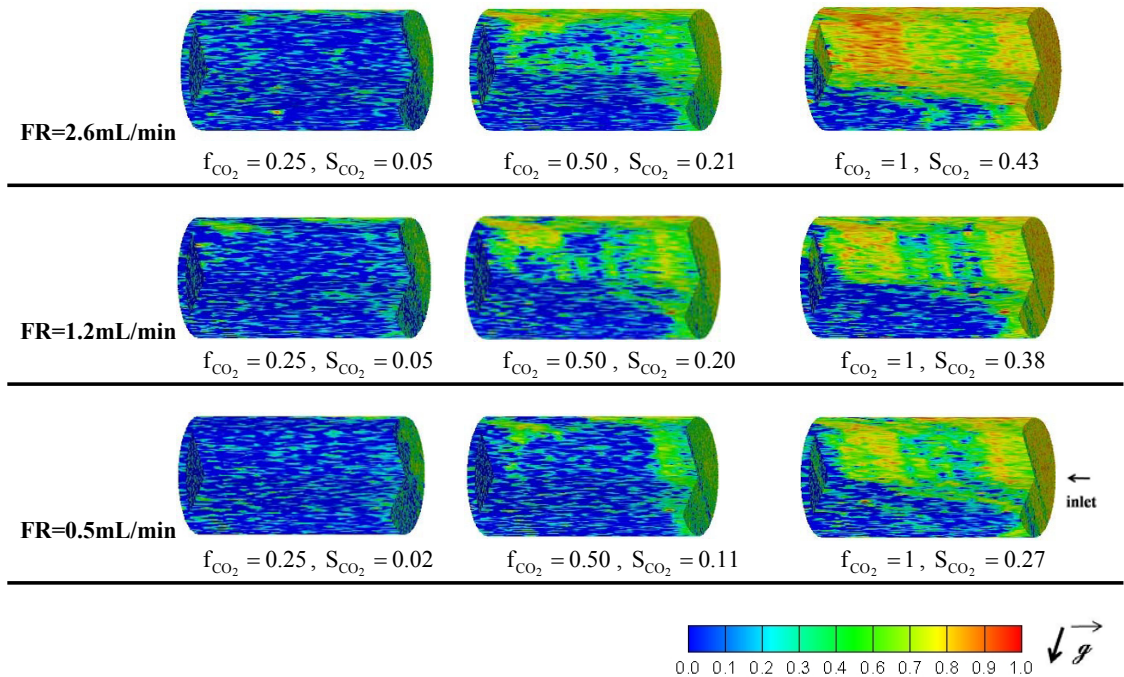


Figure 6: Three dimensional maps of CO<sub>2</sub> saturation inside the rock sample at steady state for different fractional flows of CO<sub>2</sub> and for the three different flow rates. The gravity vector is oriented as indicated by the black arrow close to the colour scale and the fluids were injected from right to left. The average CO<sub>2</sub> saturation is indicated below each image together with the corresponding fractional flow.

Relative permeability experiments have been carried out during drainage. Three different total flow rates have been used: 2.6 mL/min; 1.2 mL/min; and 0.5 mL/min. Steady state CO<sub>2</sub> saturation in the core at three different fractional flows are shown Figure 6 for the three different flow rates. Again, as in the previous example, the residual

brine saturation is high, varying from 57% at 2.6 mL/min to 73% at 0.5 mL/min. Near the core inlet there is a strong correlation between porosity and saturation distributions. Similar to the previous example, high porosity regions correspond to high CO<sub>2</sub> saturations and low porosity layers correspond to low saturations. However, this correlation is lost further in the core, which we hypothesize is caused primarily by capillary barriers created by the low porosity layers. These barriers, being oriented in the diagonal, restrict flow to the top part of the core. This effect could be enhanced by (or caused by) buoyancy induced flow because CO<sub>2</sub> has lower density than the water phase. However, since the effect of gravity should be less important for higher flow rates, the CO<sub>2</sub> saturation in the lower portion of the core would be higher in the 2.6 mL/min case in a gravity-controlled experiment, which is not observed.

Figure 7a shows the variations of the CO<sub>2</sub> saturation as a function of the total flow rate and for different fractional flows. It can be noted from this figure that CO<sub>2</sub> saturation is flow rate dependent and higher flow rate leads to a higher CO<sub>2</sub> saturation and this is true whatever the CO<sub>2</sub> fractional flow is. This effect is more important for high fractional flows. Figure 7b presents the relative permeability curves that were measured at 2.6 mL/min and at 1.2 mL/min. Note that the pressure drop across the core was too small at 0.5 mL/min to extract an accurate measure of relative permeability at this particular flow rate. The relative permeability values increase when the total flow rate increases. Drainage is thus less efficient for a lower flow rate.

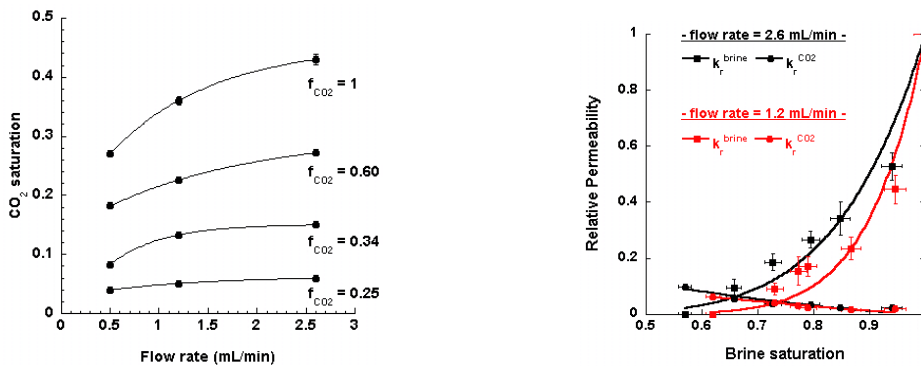


Figure 7:

a) Evolution of the CO<sub>2</sub> saturation as a function of the total flow rate for different fractional flow of CO<sub>2</sub>.

b) Relative permeability curves measured at 2.6 mL/min and 1.2 mL/min.

Co-injection of brine and CO<sub>2</sub> at  $f_{CO_2} = 0.50$  and a total flow rate of 1.2 mL/min has been simulated with the multi-phase flow simulator TOUGH2 MP. The porosity values needed for these simulations are based on the porosity maps measured by the X-ray CT scanner. Permeability values are much less certain and a number of different approaches for estimating them from the porosity data are being assessed. The Carman-Kozeny equation and a modified form of the same equation have been tested to try to reproduce the observed CO<sub>2</sub> saturation at steady state. The resulting permeability and CO<sub>2</sub> saturation maps are shown Figure 8. As seen on the figures, the permeability maps mimic the features observed in porosity distributions and enhance or reduce the contrast between high and low values, depending on the relation which is used to estimate permeability. The saturation distributions calculated with TOUGH2 MP qualitatively reproduce some of the important features in the core-flood experiments. However, bypass of the lower portion of the core observed in the experiments is not replicated. Better correlations between porosity, permeability and capillary pressure curves are being developed to improve the match between the observed and calculated saturation distributions [8].

#### 4. Conclusions

Two phase flow experiments have been performed in two different rock samples. The first experiment confirms that the spatial distribution of CO<sub>2</sub> at steady state is strongly correlated to the variation of porosity and permeability. The second drainage experiment (Berea Sandstone sample) was performed at different injection rates. The results show that both CO<sub>2</sub> saturation and relative permeability are dependent on flow rate, the displacement efficiency

being higher for a higher flow rate. The presence of heterogeneities in the sample could explain the spatial distribution of CO<sub>2</sub> in the core, as well as a combined effect of heterogeneity and gravity. Further experiments are needed to better describe and quantify this effect. Numerical simulations demonstrate that some of the features of the saturation distributions can be qualitatively replicated. However, improvements in the correlations between porosity, saturation and capillary pressure will be needed to replicate the saturation distributions measured in the experiments.

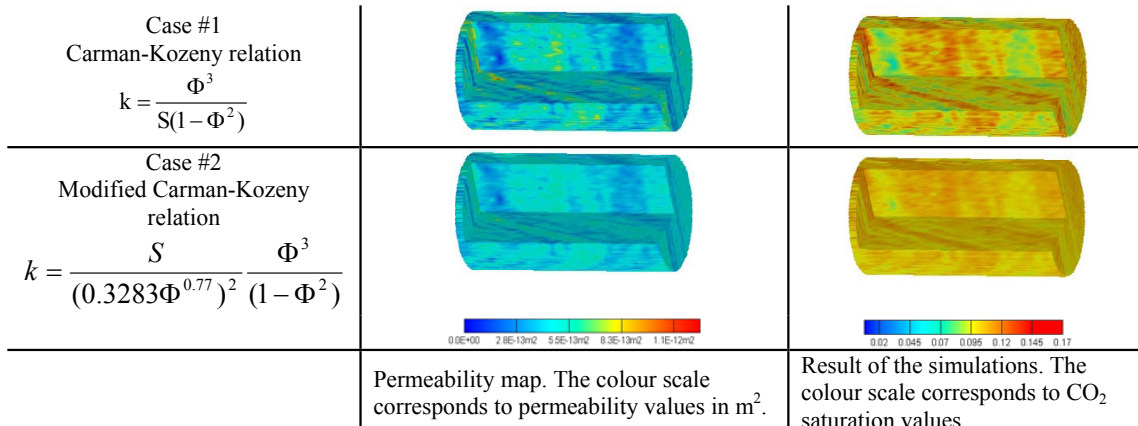


Figure 8: Left: Permeability maps obtained from the Carman-Kozeny and a modified Carman-Kozeny relation. Right: Results of the simulations.

## 5. Acknowledgements

We gratefully acknowledge the sponsors of the Global Climate and Energy Project at Stanford University, ExxonMobil, GE, Toyota and Schlumberger, for supporting this work.

## 6. References

1. Akin, S. and Kovscek, A. R., Computed tomography in petroleum engineering research, Geological Society, London, Special Publications; 2003; v. 215; p. 23-38.
2. Wellington, S. L., X-Ray Computerized Tomography, Journal of Petroleum Technology; 1987, p. 885-898.
3. Zhang, K., Doughty, C., Yu-Shu Wu, and Pruess, K., 2007 SPE Reservoir Simulation Symposium, Houston, TX; 2007.
4. Pruess, K.: "ECO2N: A TOUGH2 Fluid property module for mixtures of water, NaCl, and CO<sub>2</sub>," Lawrence Berkeley National Laboratory Report LBNL-57952, Berkeley, CA, 2005.
5. Bennion, B. and Bachu, S.; SPE 95547.
6. Benson, S.M., L. Tomutsa, D. Silin, T. Kneafsey and L. Miljkovic (2006) Corescale and Porescale Studies of Carbon Dioxide Migration in Saline Formations, Proceedings of 8th International Conference on Greenhouse Gas Control Technologies (GHGT8), IEA Greenhouse Gas Programme, Trondheim, Norway, June 19-22, 2006.
7. Miljkovic, L., Kuo, C.W., Perrin, J.J. Krause, M., and Benson, S.M., 2008. Numerical Simulations of Laboratory Core-scale CO<sub>2</sub> Displacement Experiments. Proceedings of the 9<sup>th</sup> International Greenhouse Gas Control Technology Conference, Washington, DC, Elsevier.
8. Krause, M., Perrin, J.C., and Benson, S.M., 2008. Characterization of CO<sub>2</sub> storage properties using core analysis techniques and thin section data. Proceedings of the 9<sup>th</sup> International Greenhouse Gas Control Technology Conference, Washington, DC, Elsevier.